

Article (refereed) - postprint

Cowan, N.; Levy, P.; Maire, J.; Coyle, M.; Leeson, S.R.; Famulari, D.; Carozzi, M.; Nemitz, E.; Skiba, U. 2020. **An evaluation of four years of nitrous oxide fluxes after application of ammonium nitrate and urea fertilisers measured using the eddy covariance method.**

© 2019 Elsevier B.V.

This manuscript version is made available under the CC BY-NC-ND 4.0 license <http://creativecommons.org/licenses/by-nc-nd/4.0/>



This version available <http://nora.nerc.ac.uk/525750/>

NERC has developed NORA to enable users to access research outputs wholly or partially funded by NERC. Copyright and other rights for material on this site are retained by the rights owners. Users should read the terms and conditions of use of this material at <http://nora.nerc.ac.uk/policies.html#access>

NOTICE: this is an unedited manuscript accepted for publication. The manuscript will undergo copyediting, typesetting, and review of the resulting proof before publication in its final form. During the production process errors may be discovered which could affect the content. A definitive version was subsequently published in *Agricultural and Forest Meteorology* (2020), 280: 107812. <https://doi.org/10.1016/j.agrformet.2019.107812>.

www.elsevier.com/

Contact CEH NORA team at
noraceh@ceh.ac.uk

An Evaluation of Four Years of Nitrous Oxide Fluxes after Application of Ammonium Nitrate and Urea Fertilisers Measured Using the Eddy Covariance Method

N. Cowan¹, P. Levy¹, J. Maire¹, M. Coyle¹, S.R. Leeson¹, D. Famulari², M. Carozzi³, E. Nemitz¹, U. Skiba¹

¹Centre for Ecology and Hydrology, Bush Estate, Penicuik EH34 5DR, UK

²CNR-ISAFOM, Istituto per i Sistemi Agricoli e Forestali del Mediterraneo, via Patacca 85, 80056 Ercolano, NA, Italy

³UMR EcoSys, INRA, AgroParisTech, Université Paris-Saclay, 78850 Thiverval Grignon, France

Abstract:

In this study, we present the first long-term N₂O eddy covariance dataset measured from a working farm. The eddy covariance method was used over a four year period to measure fluxes of the greenhouse gas nitrous oxide (N₂O) from an intensively managed grazed grassland, to which regular applications of ammonium nitrate or urea fertilisers were spread, for two years each at the field site. The mean emission factors (EFs) reported for ammonium nitrate and urea fertiliser applications in this study over a period of 30 days after fertilisation, were 0.90 and 1.73 % of the nitrogen applied, respectively, with EFs of individual events ranging between 0.13 to 5.71 %. Our study accurately quantifies emission factors for multiple events and showing unambiguously that large-scale variability is real. EFs do indeed vary from one fertiliser event to another, even at the same site with the same fertiliser type under similar environmental conditions. This makes distinguishing EFs between different fertiliser types for the purposes of developing emission mitigation policy very difficult.

Introduction:

Modern agriculture relies heavily upon the application of industrially produced synthetic fertilisers to provide the nitrogen (N) required for intensive crop production (Tilman et al., 2002). Global application of synthetic N fertiliser to agricultural land is now greater than 100 Tg N per year (Erisman et al., 2008). This has resulted in a large increase in emissions of the potent greenhouse gas nitrous oxide (N₂O) (IPCC, 2014). Since pre-industrial times, atmospheric concentrations of N₂O have increased by approximately 0.26 % each year (275 to over 330 ppb) as a result of human activities (Forster et al., 2007; Butler & Montzka, 2018), resulting in N₂O becoming the single largest contributor to stratospheric ozone depletion (Ravishankara et al., 2009) as well as increasing its role as a contributor to the global warming potential of the atmosphere.

35 N₂O is released after N application as a by-product of the naturally occurring microbial
36 processes of nitrification and denitrification in soils and aquatic bodies (Davidson 2000; Bateman &
37 Baggs, 2005). The microbial processes that produce N₂O are influenced by a wide variety of
38 environmental factors. Nitrification (i.e. the oxidation of ammonium) and denitrification (i.e. the
39 reduction of nitrate) rely predominantly on aerobic and anaerobic conditions, respectively (Robertson
40 & Tiedje, 1987; Davidson 2000). However, due to the heterogeneous nature of soils, the microbes
41 associated with both of these processes can coexist at a macro-scale (Anderson & Levine, 1986), so
42 the observed response to environmental variation over time can be complex. Emissions of N₂O from
43 microbial processes are known to be influenced by N availability (Cowan et al., 2017), temperature
44 (Maag & Vinther, 1996; Smith et al., 1998), pH (Stevens et al., 1998), clay content (Rochette et al.,
45 2008a) and oxygen availability, the latter of which is often controlled by soil compaction (Ball et al.,
46 1999), soil moisture and water filled pore space (WFPS) (Linn & Doran, 1984; Dobbie & Smith 2003).
47 Although relationships have been shown to exist between these soil properties and N₂O fluxes in
48 previous experiments, our understanding of the interactions with microbial activity and soil properties
49 remains poor (Butterbach-Bahl et al., 2013). As a result there are currently no process-based models
50 capable of reliably predicting microbial N₂O emissions at the field or farm scale (Brilli et al., 2017).

51 The IPCC Tier 1 method estimates the fraction of the fertiliser N that is released as N₂O after
52 a fertilisation event (the so-called “emission factor”). This is assumed to be a constant 1 % according
53 to the guidelines of the Intergovernmental Panel on climate Change (IPCC, 2014). However, there is
54 large variability and uncertainty in this value, with a reported uncertainty in the range of 0.3 – 3.0 %
55 (IPCC, 2014), and different types of fertiliser types can yield different emissions. The most common
56 form of N fertiliser is urea (over 50 % of all N applied globally), due to its high N content by weight and
57 relatively low cost (Glibert et al., 2006). Other widely used N fertiliser types include ammonium nitrate
58 (AN), calcium ammonium nitrate (CAN), ammonium sulphate, ammonium phosphate and several
59 other compounds that contain a combination of N, phosphorus and potassium.

60 The two most common synthetic N fertilizers used in the UK are AN (37.3 %) and urea (10.1
61 %) (BSFP, 2017). The application of AN, urea and CAN account for 2.2 of the 3.9 Tg of synthetic N
62 applied annually in Great Britain (BSFP, 2017). Research effort on reducing N₂O emissions has focussed
63 on quantifying the emission factors for different types of fertiliser (Smith et al., 1999; Akiyama et al.,
64 2009) to find types and application strategies which result in lower emissions.

65 The majority of studies still use the static chamber method to measure emissions, which has
66 been essentially unchanged in the last four decades (Hutchison & Mosier, 1981; Chadwick et al., 2014;
67 Flechard et al., 2007). However, because of the spatial and temporal variability in N₂O fluxes, results
68 from chamber studies have large associated uncertainties (Cowan et al., 2017). N₂O fluxes typically

69 show a highly left-skewed distribution in space, well-represented by the lognormal distribution, and
70 also resemble the lognormal density curve in time. Accurately estimating the integral under these
71 curves is very difficult with small sample sizes and infrequent sampling (Levy et al., 2017). Due to the
72 relatively large uncertainties in estimates of EFs, and the wide variety of environmental factors that
73 can influence N₂O emissions, attributing emissions to agricultural practices remains difficult. In the
74 pursuit of Tier 2 emission factors, which represent the effects of different fertiliser types in a given
75 region, better methods are required.

76 In the past, the instrumentation available to measure N₂O via the eddy covariance method
77 had been limited primarily by the sensitivities of the infra-red lasers available, requiring the use of
78 liquid nitrogen and constant alterations to hold a stable wavelength in the region required to measure
79 N₂O (Jones et al., 2011, Mammarella et al., 2010). The development of more stable laser instruments
80 has greatly improved the capability to measure N₂O in the field, particularly using the eddy covariance
81 method (Kroon et al., 2010; Haszpra et al., 2018; Liang et al., 2018; Merbold et al., 2014; Fuchs et al.,
82 2018). The eddy covariance method has several advantages which can improve estimates of emissions
83 after fertilisation events. Critically, the method allows for near-continuous measurements, that
84 integrates emissions from a relatively large spatial region (> 100 m) (Vesala et al., 2008). This method
85 can thereby remove the uncertainties in upscaling measurements to the field scale, and provide more
86 defensible estimates of cumulative flux emissions.

87 This study presents a long term dataset of N₂O fluxes measured using the eddy covariance
88 method from a grazed grassland field in Scotland (Easter Bush). This is the longest eddy covariance
89 dataset of N₂O from a working farm we know of to date. The measurements cover four growing
90 seasons, during which, AN fertiliser was applied for two seasons (2012 and 2018) and urea fertiliser
91 was applied for two seasons (2016 and 2017). The aim of this manuscript is primarily to present
92 methods for estimating emission factors using eddy covariance observations, and to compare the
93 emissions associated with each of the fertiliser types, with associated uncertainties.

94

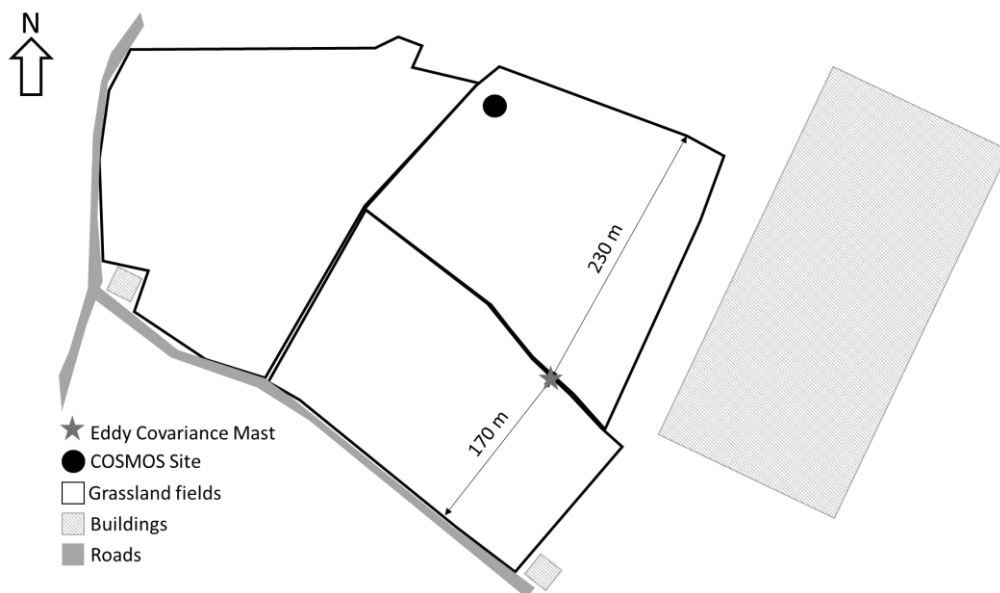
95 **Method:**

96 Field site and management

97 Measurements were made at the permanent Easter Bush field site in the Easter Bush Estate
98 (Midlothian, UK, 55°51'57.4"N 3°12'29.3"W) (Cowan et al., 2016; Jones et al. 2017) during 2012, then
99 in 2016, 2017 and 2018. The site consisted of a small enclosed area in which a permanently stationed,
100 temperature controlled cabin with access to mains power was located directly between two similarly
101 managed grazed grasslands (North and South fields, each approximately 5.4 ha, Figure 1). The soil in
102 the fields are classed as an imperfectly drained clay loam with a sand/silt/clay texture of 26/20/55 in

103 the top 30 cm. The grassland fields had been predominantly used as high intensity grazing pasture for
104 sheep (0.7 LSU ha^{-1}) for over twenty years before measurements took place, with occasional silage
105 harvest. Their management is typical for this region, with predominately AN fertilization (but urea was
106 used for two years during this study) via tractor mounted broadcast spreading, with liming every 3-5
107 years to maintain the pH between 5.5 and 6 and occasional ploughing and reseeded.

108 The sheep were typically absent from the fields in the winter months (November to February),
109 with sporadic movement between local fields throughout the growing season (March to September)
110 as management required. Both fields were managed similarly across the measurement period with
111 sheep grazing throughout the year, although there were stages when field management differed
112 (Table 1). Fertiliser was applied to both fields on the same days with the same quantities throughout
113 the growing seasons (Table 1). In 2012 there was a tillage event in the south field, thus the fields
114 cannot be classed as similar in this period. For this reason we split flux measurements between the
115 fields in 2012, with only the north field receiving a fertiliser application during event 1, and both fields
116 receiving similar applications during the second event. As the wind shifted regularly to and from the
117 predominant south westerly direction to a north easterly direction during 2012, we can observe the
118 effects from both fields separately. For all other events (2016 to 2018), both fields were managed
119 similarly and measurements from both fields are considered as one event.



120
121 **Figure 1** The eddy covariance mast and meteorological measurement equipment were positioned in
122 a small enclosed area between two grazed grassland fields at the Easter Bush permanent field site,
123 Midlothian, Scotland, UK.

124

125 **Table 1** Field management and fertiliser application for the North and South fields during eddy
 126 covariance measurements at the Easter Bush permanent field site.

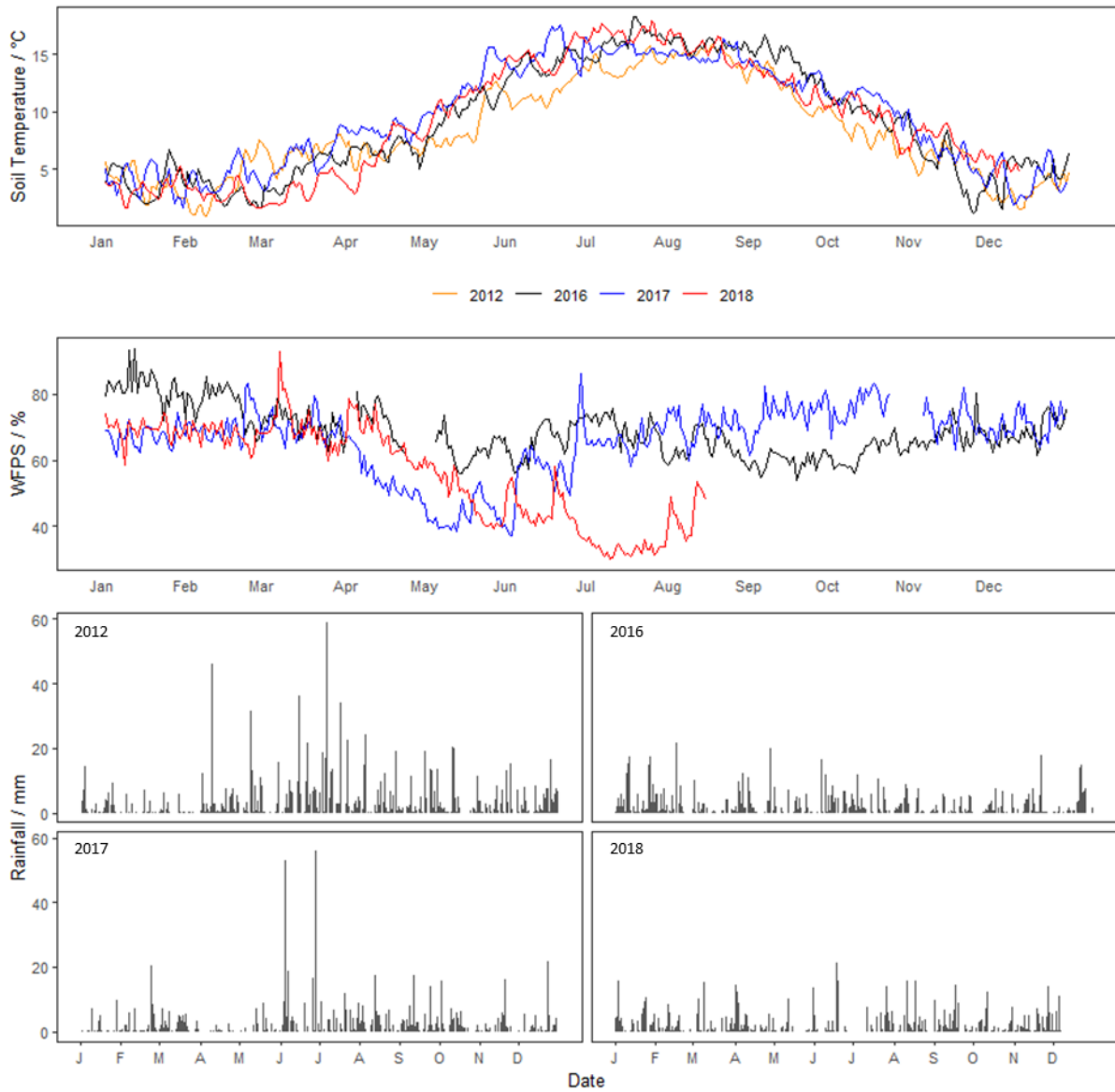
Date	Field	Management	Fertiliser Application
01/05/12	South	Tilled and resown	
28/05/12	North		AN 70 kg N ha ⁻¹
09/08/12	Both		AN 70 kg N ha ⁻¹
20/05/14	North	Tilled and resown	
15/03/16	South	Sheep removed	
13/06/16	Both		Urea 70 kg N ha ⁻¹
16/07/16	South	Silage harvest	
26/07/16	Both		Urea 50 kg N ha ⁻¹
28/07/16	South	Sheep returned	
23/08/16	Both		Urea 35 kg N ha ⁻¹
01/04/17	Both		Urea 70 kg N ha ⁻¹
22/06/17	Both		Urea 49 kg N ha ⁻¹
12/04/18	Both		AN 70 kg N ha ⁻¹
14/06/18	Both		AN 52 kg N ha ⁻¹

127

128 Meteorology and Environment

129 Measurements of soil temperature (0.35 m depth), air temperature (1.8 m height) and rainfall (tipping
 130 bucket) were made at the field site throughout the measurement period and averaged every 30 min
 131 (Figure 2, Table 2). After installation in 2015, soil moisture (0 – 30 cm) was also measured by a cosmic-
 132 ray moisture sensor (Hyroinnova CRS-2000) (Köhli et al., 2015) at the COSMOS-UK Easter Bush
 133 measurement site (<https://cosmos.ceh.ac.uk/>), located approximately 300 m north of the flux mast
 134 (Figure 2). Temperatures were not drastically different at the site during the growing seasons that flux
 135 measurements took place; however, 2012 was consistently cooler than the other years during the
 136 summer months (June to August). Soil moisture measurements were not available in 2012 as the
 137 COSMOS instrument was not installed until 2015. Rainfall was significantly higher than what is
 138 considered typical of the site in the summer of 2012, with an annual rainfall of 1191 mm. Total annual
 139 rainfall for the other years was 793, 780 and 690 mm for 2016, 2017 and 2018 (up to 12/12/18),
 140 respectively. A drought occurred during May in 2017, and more severely during the summer of 2018
 141 (July) after a particularly cold spring. During these periods (April to May in 2017 and May to September
 142 in 2018) the soil became very dry and field scale water filled pore space (WFPS %) of the soil dropped
 143 below 40 %.

144



145

146 **Figure 2** (top) Daily average soil temperature (0.35 m depth), (middle) Hourly soil moisture (0 – 30 cm

147 depth) expressed as WFPS % by COSMOS instrument (bottom) Daily cumulative rainfall.

148

149

150 **Table 2** Measured environmental variables were averaged/summed for 7 and 30 day periods prior to
 151 and post fertilisation events. Soil moisture measurements were not available in 2012.

152

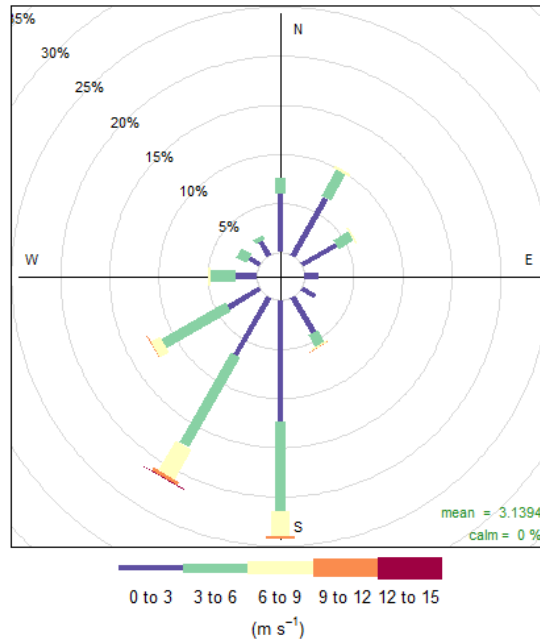
Year	2012	2012	2016	2016	2016	2017	2017	2018	2018
Event	1	2	1	2	3	1	2	1	2
30 days prior									
Mean air temperature (°C)	8.3	13.3	10.9	14.3	14.3	7.0	14.6	4.2	12.3
Mean soil temperature (°C)	8.3	14.4	12.3	15.9	16.1	6.0	14.8	4.0	13.3
Mean soil moisture (WFPS %)	NA	NA	62.5	70.4	65.7	70.0	51.8	68.8	45.0
Cumulative rainfall (mm)	92.0	148.1	59.2	69.4	60.6	59.0	114.6	72.0	31.4
30 days post									
Mean air temperature (°C)	11.2	14.5	12.8	14.3	14.5	7.7	13.3	9.5	14.6
Mean soil temperature (°C)	11.5	14.5	14.8	16.0	15.3	8.4	15.5	8.4	15.7
Mean soil moisture (WFPS %)	NA	NA	70.8	65.2	60.4	55.5	64.0	60.9	39.5
Cumulative rainfall (mm)	152.8	81.8	85.2	52.8	26.6	6.6	116.8	31.6	49.8
7 days prior									
Mean air temperature (°C)	14.5	14.1	12.4	16.8	14.9	9.3	16.4	6.6	12.9
Mean soil temperature (°C)	11.2	15.0	14.5	17.5	16.0	7.2	16.5	4.7	14.9
Mean soil moisture (WFPS %)	NA	NA	62.9	67.8	65.9	69.0	56.4	71.8	42.6
Cumulative rainfall (mm)	0.2	40.5	34.6	20.2	12.6	4.6	11.6	18.4	5.0
7 days post									
Mean air temperature (°C)	10.3	15.7	11.6	13.8	14.6	8.5	12.3	9.3	11.5
Mean soil temperature (°C)	11.5	15.2	13.5	16.5	15.6	8.3	15.5	6.7	13.6
Mean soil moisture (WFPS %)	NA	NA	70.3	65.0	62.9	64.9	56.6	68.4	45.2
Cumulative rainfall (mm)	19.6	9.9	28.2	5.4	0.8	0.0	34.8	9.8	40.8

153

154 Eddy covariance measurements

155 An eddy covariance mast was erected in an enclosure between the North and South fields (see Figure
 156 1). The mast was equipped with an ultra-sonic anemometer (WindMaster Pro 3-axis, Gill, Lymington,
 157 UK) mounted at a height of 2.5 m to measure fluctuations in 3-D wind components at a frequency of
 158 20 Hz. The prevailing wind direction was SW-NE, with predominant SW winds, however the wind field
 159 did vary on a number of occasions throughout the four years of measurement (see Figure 3). A 14 m
 160 length of 1/4" ID Dekabon tubing was attached to the mast near the sonic anemometer (northward,
 161 eastward and vertical separation from the centre of the sonic of 14, 4 and 15 cm, respectively). This
 162 inlet was run back along a protected conduit into the temperature controlled cabin where it was
 163 connected to a continuous wave quantum cascade laser (QCL) absorption spectrometer gas analyser
 164 (CW-QC-TILDAS-76-CS, Aerodyne Research Inc., Billerica, MA, USA). A 1 µm PTFE membrane air filter
 165 was fitted in-between where the inlet line joined the QCL to prevent particulates from damaging the
 166 instrument.

167 The QCL was fitted with either one of two different laser sources over the four year period,
168 each capable of measuring atmospheric N₂O with an instrumental noise smaller than 0.3 ppb, together
169 with H₂O and either CO₂ or CO, using absorption features in the mid-infrared spectral range close to
170 2200 cm⁻¹. The TDLWintel software (Aerodyne Research Inc., Billerica, MA, USA), fits the observed
171 spectra to a template of known spectral absorption line profiles from the HITRAN (High-resolution
172 TRANsmission) molecular spectroscopic database. Absolute trace gas mixing ratios can then be
173 calculated from the intensity of the absorption line measured, the temperature and pressure of the
174 absorption cell and the optical path length with an accuracy within 3 %. A vacuum pump (Triscroll 600,
175 Agilent Technologies, US) was used to draw air through the inlet and instrument with a flow rate of
176 approximately 14 l min⁻¹. Data from the sonic anemometer and QCL were logged synchronously using
177 a custom-made program written in LabView™ (National Instruments, TX, USA).
178



Frequency of counts by wind direction (%)

179

180 **Figure 3** Wind rose measured at the Easter Bush site for the duration of all eddy covariance
 181 measurements.

182

183 Fluxes were calculated over 30 minute intervals using the EddyPro software (Version 6.2.1, Li-
 184 COR, Lincoln, NE, U.S.A.), based on the covariance between gas concentration (χ) and vertical wind
 185 speed (w) ($F\chi = \overline{\chi'w'}$). For flux data taken with a low signal-to-noise ratio, time lag identification by
 186 maximisation of the covariance between χ and w introduces systematic biases (Langford et al., 2015).
 187 Instead, the time lag was estimated on a six hour basis for N₂O, taking the maximisation of covariance
 188 of data over six hours of measurement data. Firstly, all six hour data chunks were given a 10 second
 189 window to find the maximisation of covariance. Time lag varied through the years as the different
 190 instruments were swapped in and out of the enclosure (mode time lag varied between 1.1 to 1.4 s for
 191 all setups based on changes made to tubing and filters), although once running undisturbed, the mode
 192 time lag remained very consistent for extended periods (less than 0.1 s drift over 6 months). A second
 193 maximisation of covariance was carried out once a stable (mode) time lag had been identified. Here
 194 we ran the maximisation of covariance of the six hour data chunks a second time, constrained to within
 195 a 0.2 second window around the mode time lag we observed in the initial analysis. This time lag was
 196 then fixed for all data within the six hour chunk and fluxes were calculated on a 30 minute basis. This
 197 method was verified by comparing N₂O time lag with CO₂ time lag for the periods in which CO₂
 198 measurements were available (2012 and late 2018), which were almost identical.
 199 In the flux calculation processing, we applied double coordinate rotation (vertical and crosswind),
 200 spike removal, block averaging and outlier removal of artefact measurements. Correction for the

201 frequency response of the system, both high and low-frequency losses, were made using the analytical
202 method of Moncrieff et al. (1997). Corrections for density fluctuations due to temperature fluctuations
203 were applied on a half-hourly basis using the method of Ibrom et al. (2007). The quality control scheme
204 of Foken (2003) was used to remove poor quality flux measurements (category 5 or above). Data were
205 also rejected on the basis of extreme outliers and friction velocity (u^*) values less than 0.1 m s^{-1} . Only
206 data in which at least 90 % of the flux came from a radius of 200 m from the flux tower and data in
207 which the peak contribution to the flux was at least 25 m from the tower were used in this study,
208 based on the calculations of Kjun et al. 2004. Flux random uncertainty was estimated by the method
209 of Finkelstein and Sims (2001) integrated over a fixed 10 s correlation period (as presented in Figures
210 5 and 6). This was chosen because the estimation methods of the integral time scale of the turbulence
211 become uncertain for noisy data.

212

213 Estimating cumulative fluxes and emission factors (EFs)

214 After quality control (i.e. removal of data where there was a lack of turbulence or there were technical
215 difficulties with instrumentation), a significant portion of the data was removed from the final results.
216 Over the four years, 35 % of the recorded data (during periods where there were no technical faults)
217 passed quality control steps. In order to estimate cumulative fluxes, interpolation of the missing data
218 points was required. However, in the absence of a well-validated process-based model for N_2O fluxes
219 on which to base predictions, it is not obvious how this is best achieved. To this end, we used a
220 smoothing approach via a general additive model (GAM). This accounted for temporal patterns at a
221 range of time scales and nonlinear responses to environmental variables, implemented using the mgcv
222 package in the R software (Wood, 2006). The GAM was fitted to the flux data, using the same model
223 terms for both the AN and Urea events over the four year period (with the exception of 2012 for which
224 no soil moisture data was available). The terms included were soil temperature, precipitation, soil
225 moisture (measured by the COSMOS system) and time since fertilisation. The GAM allows for non-
226 linearity by fitting a smooth response with cubic splines. The degree of smoothing is optimised by the
227 algorithm, but was also adjusted subjectively, such that the model was not over-fitting to noise in the
228 data. The emission factor (EF) for each event was calculated as the cumulative flux of N_2O over 30
229 days after fertilisation, divided by the quantity of total nitrogen applied. As a single eddy covariance
230 tower is unable to make measurements of background flux in tandem with the experimental
231 measurements, we do not negate background flux from our EFs in this study. Uncertainty was
232 quantified by simulating 2000 replicate time series from the GAM, given the uncertainty in the fitted
233 parameters, to estimate the posterior distribution. The quantiles of this posterior distribution
234 provided the 95 % credibility interval at each predicted time step (Marra and Wood, 2012). Finally, the

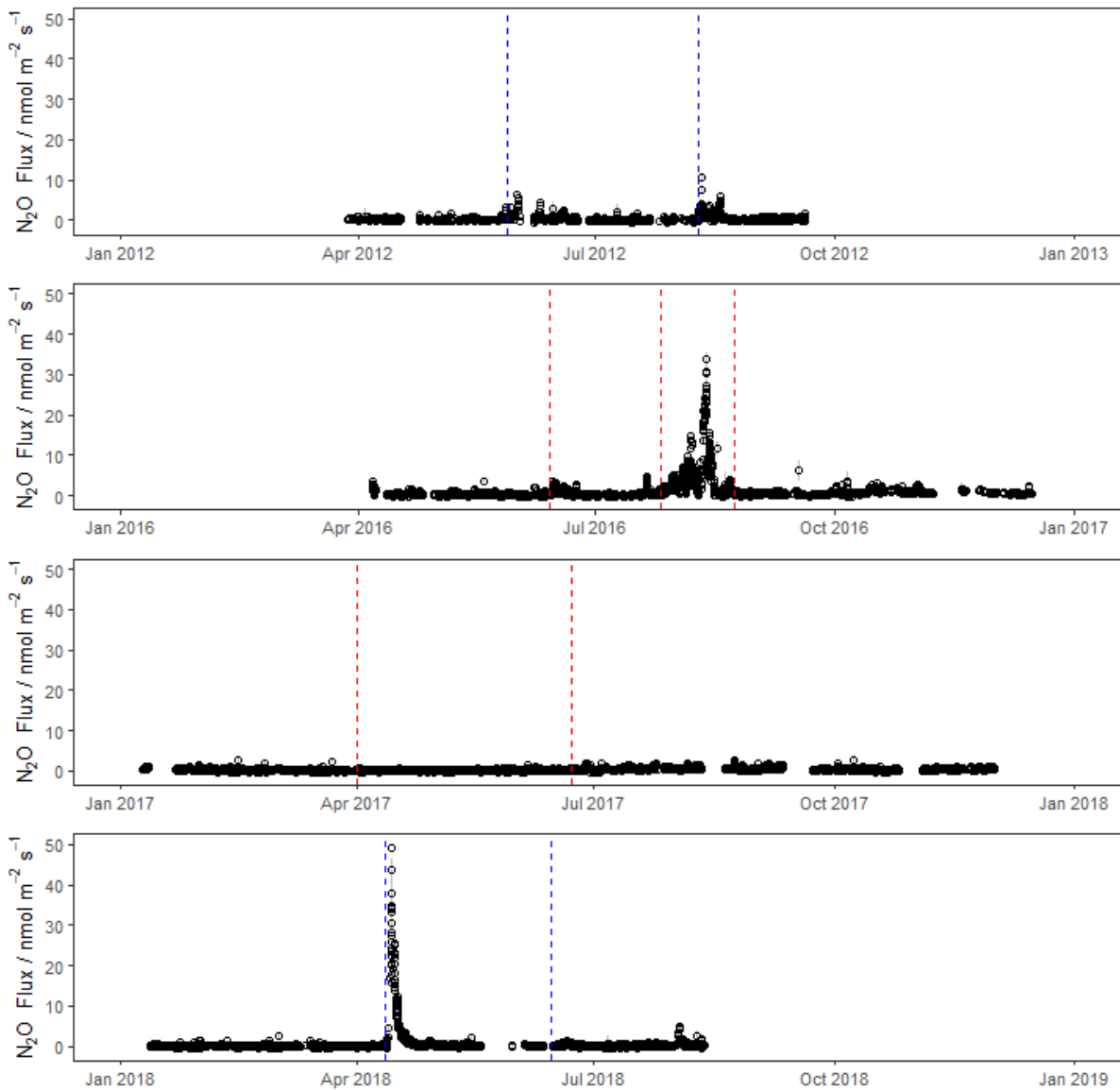
235 correlations between the N₂O emission and the environmental variables have been evaluated with t-
236 Test for independent samples (R core team).

237

238 **Results:**

239 Eddy covariance measurements of N₂O

240 With the exception of the fertilisation events, emissions of N₂O from the grasslands generally
241 remained close to zero ($< 1 \text{ nmol N}_2\text{O m}^{-2} \text{ s}^{-1}$, ($< 28.01 \text{ ng N}_2\text{O-N m}^{-2} \text{ s}^{-1}$)), even with the presence of
242 grazing sheep which produce a continuous input of urine and faeces and should increase N₂O
243 emissions (Figure 4). After N fertiliser was applied, it was typical to see an immediate increase in
244 emissions, reaching a peak within 7 days, with a return to fluxes near zero after two to three weeks.
245 It is evident from these measurements that the application of fertiliser is the main cause of N₂O
246 produced in the fields and that the vast majority of emissions occur within 30 days after the application
247 (Figure 4). There was no obvious pattern among fertiliser events related to fertiliser type or quantity
248 of N applied (see Table 1 for details). After fertiliser events, emissions ranged from approximately zero
249 (2017), to extreme spikes in emissions reaching fluxes greater than $40 \text{ nmol N}_2\text{O m}^{-2} \text{ s}^{-1}$ (2018). The
250 shape of the peak also varies between events: we observed both the expected sharp rise and gradual
251 fall (2018, AN Event 1) and also a gradual rise and sharp fall (e.g. 2016, urea Event 2).

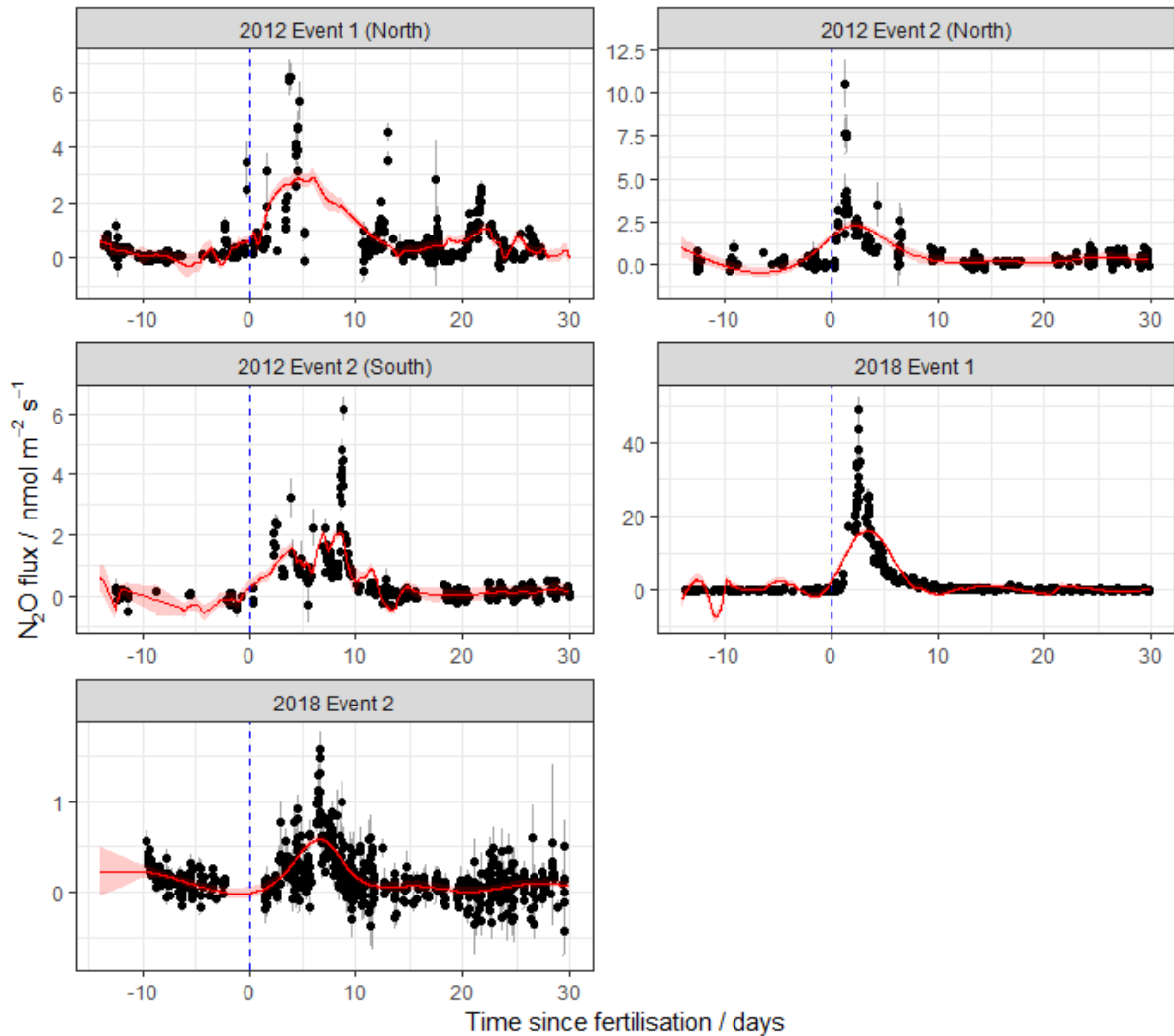


252
 253 **Figure 4** Fluxes of N_2O measured using the eddy covariance method over four years at the Easter Bush
 254 field site (Midlothian, Scotland, UK). AN fertiliser (blue) was applied in 2012 and 2018, and urea
 255 fertiliser (red) was applied in 2016 and 2017 (dashed vertical lines show fertiliser application dates
 256 described in Table 1). This data is not gap-filled.

257 As the majority of emissions appear to occur within one to three weeks after each fertilisation
 258 event, and that fertiliser events often occur in fairly short succession, in this study we limit emissions
 259 associated with each event to 30 days after application for comparison purposes.

260 For the events in which AN was applied, emissions of N_2O generally followed the typical rise
 261 and fall of emissions expected after N application (Figure 5). The magnitude of fluxes observed after
 262 each fertiliser event varies greatly. The smallest of peaks after AN application was observed in 2018
 263 (Event 2), but a pronounced peak was still visible after the fertiliser application.

264



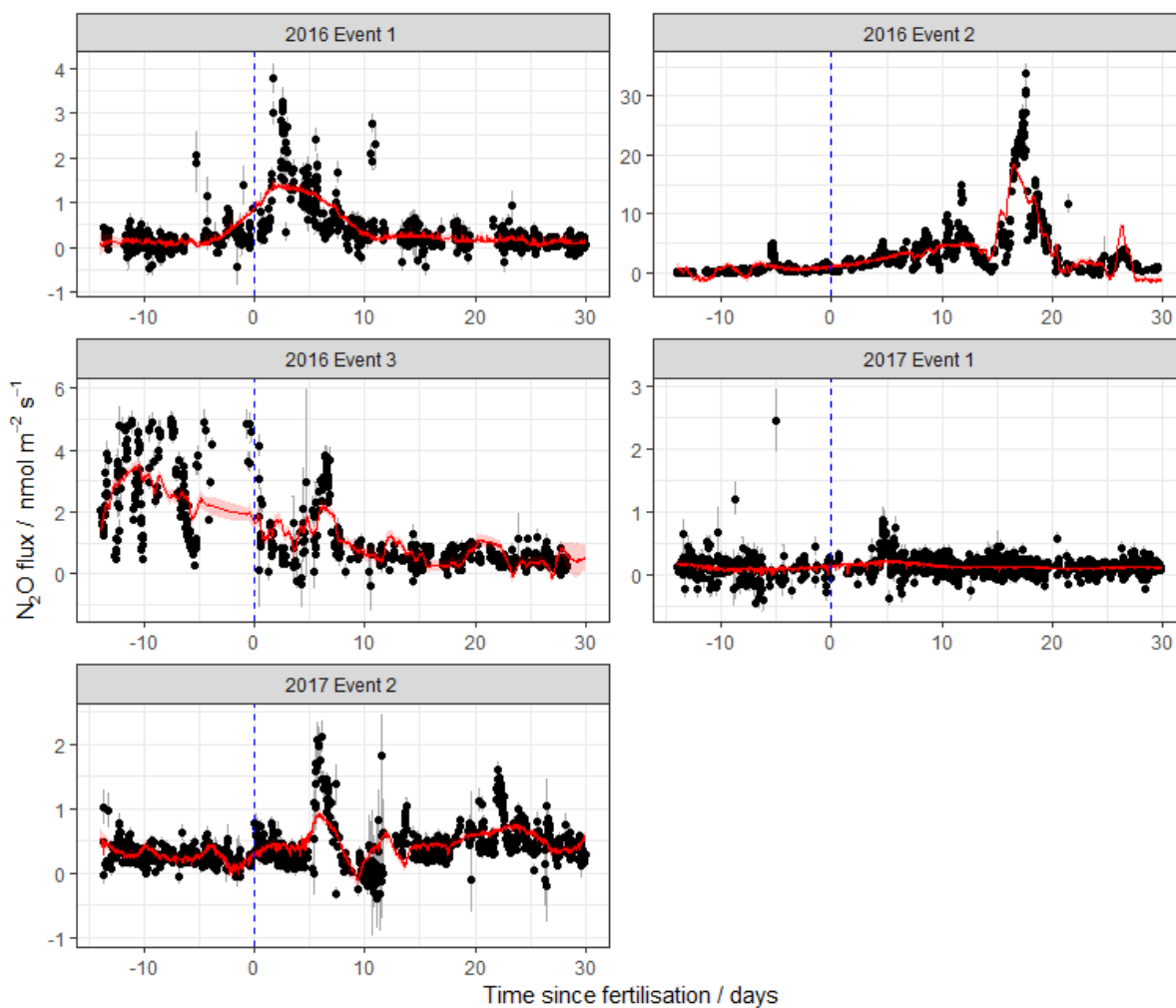
265

266 **Figure 5** Emissions of N_2O measured 14 days before and 30 days after the application of AN fertiliser.
 267 (Due to the tillage event occurring in 2012, the two adjacent fields are treated separately). The GAM
 268 interpolation (Red) and associated 95 % confidence intervals (C.I.s) are fit to the data for each event.
 269 The date of the fertiliser event is shown by the dashed vertical line.

270

271 For the events in which urea was applied (Figure 6), the patterns in emissions were more
 272 varied. The largest emission after a urea application (2016, Event 2) appeared to have a delay, peaking
 273 16 days after application. Fluxes after the events in 2017 were similar in magnitude to background
 274 emissions, with only small peaks observed.

275



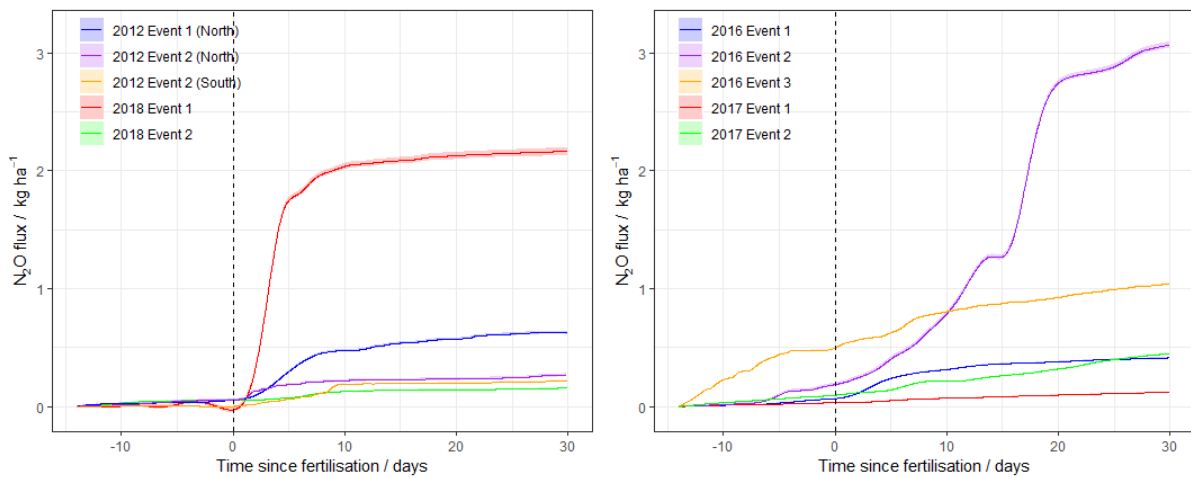
276

277 **Figure 6** Emissions of N₂O measured up to 30 days after the application of urea fertiliser. The GAM
 278 interpolation (Red) and associated 95 % confidence intervals (C.I.s) are fit to the data for each event.
 279 The date of the fertiliser event is shown by the dashed vertical line.

280

281 Cumulative fluxes of N₂O over a 30-day period after a fertiliser event ranged from 0.092 to
 282 2.856 kg N ha⁻¹ (Figure 7, Table 2). Cumulative fluxes varied widely for both of the different fertiliser
 283 types, with one very large emission event each. In most events, pre-fertilisation fluxes were negligible,
 284 with the exception of the 2016 Event 3 urea application, which was close in time to the previous
 285 fertiliser application. Emission factors reported in this study range from 0.13 to 5.71 % (Table 3).
 286 Emission factors for AN and urea showed no clear difference, and had similar variability: the mean EFs
 287 were 0.90 (s.d. ± 1.08) and 1.73 (s.d. ± 2.30) %, respectively. The mean EF for urea in this study was
 288 dominated by one event (2016 Event 2), which tails off into the next urea application event (2016
 289 Event 3). Because observations have near-complete temporal coverage and measure a spatial
 290 average, we have a high degree of confidence in the emission factor for individual events (as shown

291 in Figure 7). However, there is wide variability among events which is not explained by fertiliser type,
 292 and we are therefore very uncertain of the mean effect of AN or urea.
 293



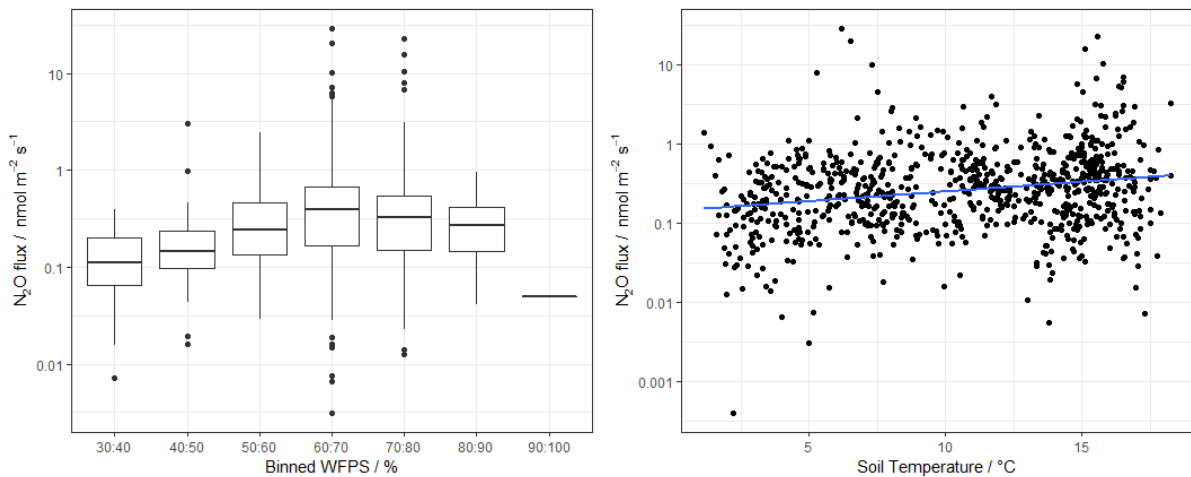
294
 295 **Figure 7** Cumulative fluxes are calculated 14 days before and 30 days after the application of AN
 296 (left) and urea (right) applications. The GAM method is used to interpolate measurement data and
 297 estimate 95 % C.I.s in cumulative flux estimates (shaded).

298 **Table 3** Cumulative fluxes over a 30-day period after each fertilisation event are reported for the GAM
 299 method (units in kg N₂O-N ha⁻¹). The 95 % confidence intervals (C.I.s) are included for comparison.

Year	Event	Fertiliser Applied	N ₂ O Flux 30 day Cumulative kg N ₂ O-N ha ⁻¹	± 95 % C.I. kg N ₂ O-N ha ⁻¹	Emission Factor %
2012	1 (North)	AN 70 Kg	0.650	0.004	0.93
2012	2 (North)	AN 70 Kg	0.203	0.003	0.29
2012	2 (South)	AN 70 Kg	0.224	0.003	0.32
2016	1	Urea 70 Kg	0.325	0.002	0.46
2016	2	Urea 50 Kg	2.856	0.009	5.71
2016	3	Urea 35 Kg	0.582	0.004	1.66
2017	1	Urea 70 Kg	0.092	0.001	0.13
2017	2	Urea 49 Kg	0.341	0.001	0.70
2018	1	AN 70 Kg	1.944	0.013	2.78
2018	2	AN 52 Kg	0.103	0.001	0.20

300
 301 Environmental impacts on N₂O emissions
 302 The available environmental variables of precipitation, soil moisture (0 – 30 cm) and soil and air
 303 temperature were investigated for correlation with N₂O emissions over the four years of
 304 measurements. Log-transformed daily-mean fluxes correlated significantly with soil moisture and soil
 305 temperature (P << 0.01); however, there remains a large amount of scatter in these relationships
 306 (Figure 8). A bell-curve relationship is observed with the fluxes and soil moisture, peaking at 60 – 70

307 % WFPS, and it appears that there is a small increase in N₂O flux with temperature. Neither of these
 308 relationships, nor multiple regressions with all environmental variables provides a useful predictor of
 309 emissions of N₂O. No diurnal cycling in emissions was observed, suggesting temperature changes
 310 between day and night had no significant impact of flux measurements. A comparison of EFs with
 311 environmental properties revealed no strong correlation between emissions and environmental
 312 conditions when looking at 7 or 30 day periods before and after fertiliser application (Table 2),
 313 although the WFPS % at the date of fertilisation was deemed significant (P =0.04) in a multiple
 314 regression fit (using the lm function in the 'stats' package for the statistical program R) with mean soil
 315 temperature, mean WFPS % and cumulative rainfall over 30 days (R² = 0.65). However, this fit is
 316 dominated by a single point (the large 5.71 % EF) and no correlation with any variables is found when
 317 it is removed.
 318



319 **Figure 8** (left) A boxplot of N₂O on a log scale against WFPS binned by 10 % groups. The boxplot shows
 320 the median with hinges on the 25 % and 75 % quantiles. (right) Linear regression between N₂O on a
 321 log scale and soil temperature (line).
 322

323

324

325 **Discussion:**

326 Measurements of N₂O using the Eddy Covariance Method

327 The advantage of using the eddy covariance method to measure N₂O fluxes is the near-continuous
 328 data coverage, paired with the spatial integration (covering up to several 100 m²). This provides a
 329 detailed picture of N₂O flux at the field scale throughout the four-year measurement period with
 330 limited logistical effort (i.e. no intensive field work is required to carry out measurements after
 331 fertiliser events). Even the most rigorous of manual chamber sampling schedules accounts for just a
 332 few m² with intermittent timings between measurements (mostly done during the day). Using the

333 eddy covariance method we can mitigate the uncertainty arising from spatial and temporal
334 heterogeneity at the field scale, which is notoriously high and difficult to deal with using chamber
335 measurements (Rochette et al., 2008b; Levy et al., 2017). However, with the eddy covariance method,
336 it is also difficult to determine the influence of environmental conditions as a direct comparison
337 cannot be made between two fertiliser treatments or a control when using one tower. Unless multiple
338 towers are deployed in parallel fields, the eddy covariance method cannot assess fertiliser treatments
339 in tandem.

340 Emissions observed from the fields were most varied after N application, for which fluxes
341 varied log-normally over time, as is often observed with eddy covariance (Jones et al., 2011; Merbold
342 et al., 2014; Liang et al., 2018) the flux-gradient method (Wagner-Riddle et al., 2007; Glenn et al.,
343 2012; Abalos et al., 2015; Waldo et al., 2019) and chamber methods (Levy et al., 2017). Although each
344 30-minute flux measurement represents a large footprint ($> 100 \text{ m}^2$), there remains some spatial
345 variability in the reported measurements because the method is reporting measurements weighted
346 towards a particular part of the field at any given time, depending on wind speed and direction. As the
347 wind direction was predominantly south westerly during measurements (see Figure 3), this section of
348 the field dominates the contributions to the measurements in this analysis. With the exception of a
349 two month period in May to June in 2012 when the south field was tilled and re-sown (north field was
350 tilled and re-sown in 2013 between measurement periods), both fields were in a permanent state of
351 full grass coverage.

352 As fluxes seemed uncharacteristically low after fertiliser applications in 2017, further checks
353 were carried out to ensure that the system was still operating as normal. The reasons for this lack of
354 N_2O emission is unclear, as rainfall and temperatures were not abnormal during the growing seasons
355 or the periods in which fertiliser was applied. Although there was limited rainfall in the immediate
356 days after the first fertiliser event in 2017 (see Table 2), the WFPS of the soil was relatively high due
357 to the high rainfall that preceded it. The urea pellets were readily dissolved by the damp surface and
358 the formation of morning dew which forms regularly at the site in the cool damp climate. The EF of
359 the second event in 2017 was also low, and did not respond to higher rainfall as may be expected. The
360 reason for these observations is unclear.

361 As the laser source in the QCL instrument also measured H_2O and CO in tandem with N_2O , we
362 checked fluxes measured in 2017 and compared them with those measured in 2016. There were no
363 significant changes in fluxes of H_2O and CO between the times that high N_2O fluxes were observed in
364 2016 with comparison to the low fluxes observed in 2017; therefore we conclude that the low fluxes
365 of N_2O in 2017 are genuine (CO fluxes for this period are published in Cowan et al., 2018). Other factors
366 such as vegetation height or plant uptake should not have impacted EFs as the grass height of the

367 grazed pasture was fairly consistent across the duration of all years, with the exception of the silage
368 cut in 2016.

369 Rather than the low emissions from 2017 seeming suspect, it is perhaps the large emission
370 event after the second application of urea in 2016 that is not representative. During the four years of
371 measurements, there was only one harvest of silage from the field, approximately one month before
372 the high flux event in 2016. Based on previous experimentation at the site, which found high emissions
373 of N₂O approximately one month after a tillage event in which the grassland crop was ploughed into
374 the soil (Cowan et al., 2014), we speculate that the high emissions in 2016 may be the result of a large
375 mass of decaying crop residue. Based on estimates made by the farm manager, automated collection
376 methods of silage grass can expect to miss up to 10 % of a harvest. The decay of this crop residue and
377 mineralisation of nitrogen into the soil may have resulted in an additional N input, and thereby
378 impacted the EFs for events 2 and 3 in 2016. If these events were excluded, this would bring the mean
379 emission factor for urea down to 0.43 % which is in line with other studies carried out at the site
380 (Cowan et al., 2019).

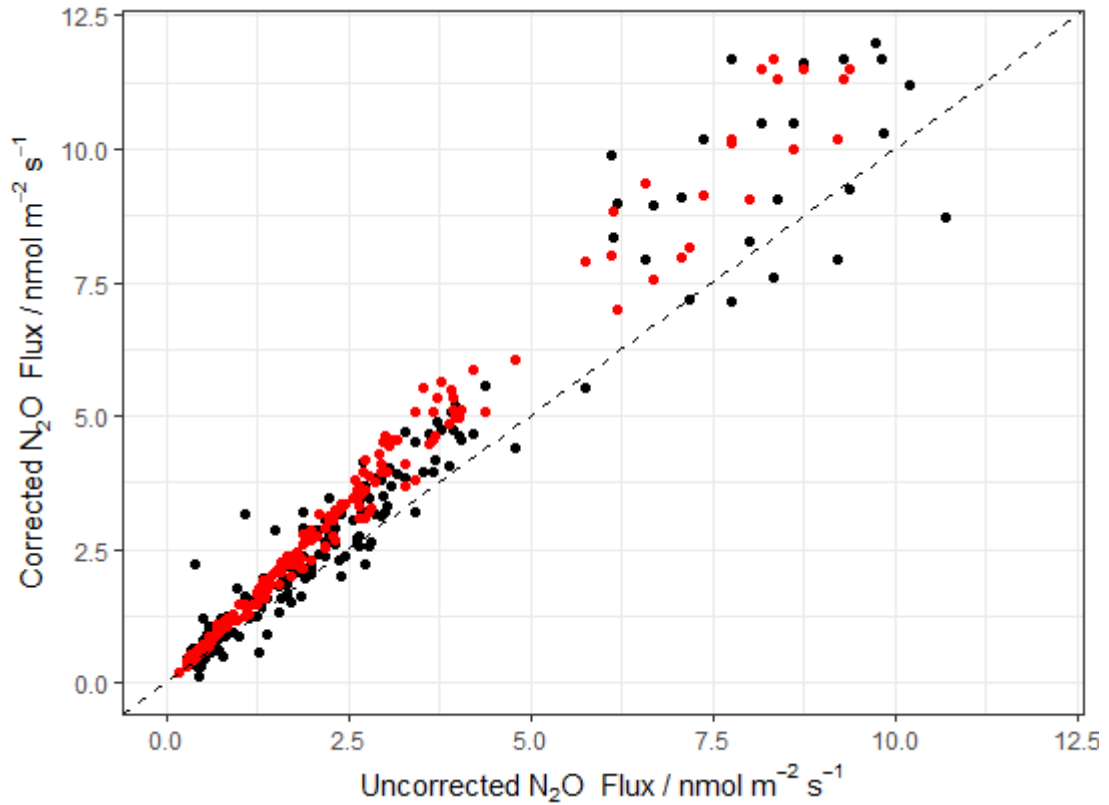
381

382 Flux Data Interpolation

383 Interpolation of data measured using the eddy covariance data is considerably less of a problem here
384 than when using the flux chamber approach. Gap filling N₂O fluxes using the GAM method suits the
385 eddy covariance method well when there are few missing data points. In this study, the relatively high
386 data coverage, with limited gaps spanning more than a few hours, considerably reduces the
387 uncertainty. Due to the large number of points to which the GAM is fit, the uncertainties calculated
388 are very small, but these do not account for two important factors: (i) any systematic uncertainties
389 which may be present in the eddy covariance method are ignored, and (ii) autocorrelation (and
390 thereby non-independence) of the samples in the time series is not considered.

391 At our field site in particular, the short height of the mast (< 3m) paired with the cold weather
392 limit our ability to consistently measure well-formed spectra of sensible heat. This presents issues
393 when correcting for high frequency losses which can systematically impact flux calculations. In our
394 study we default to the Moncrieff et al., (1997) method to perform these corrections as applying the
395 more defensible Fratini et al., (2012) method which requires well-formed sensible heat spectra to
396 account for the effects of relative humidity in closed-path systems was not possible to achieve
397 consistently across the four years. By comparing fluxes calculated using both methods during a period
398 that sensible heat measurements were available and fluxes ranged from high to low (16/04/18 to
399 23/04/18), we can see that differences in overall flux estimates are only fractional (Figure 9; R² =
400 0.975); however, the Moncrieff method appears to underestimate fluxes (~ 10 %) when emissions are

401 high ($> 8 \text{ nmol m}^{-2} \text{ s}^{-1}$). As less than 1% of observed fluxes past beyond this threshold, this effect is
402 unlikely to have a large impact on cumulative emissions over long periods of time, but may alter EFs
403 calculated after particularly high and short-lived emission events (such as 2016 Event 2 and 2018 Event
404 1).



405
406 **Figure 9** High and low-frequency losses, were corrected for using the analytical method of (Moncrieff
407 et al. (1997, black). Potential systematic uncertainties may influence flux calculations depending on
408 the exact method used, as demonstrated by comparing our results with those estimated using the
409 method of Fratini (et al., 2012, red) for the period 16/04/18 to 23/04/18.

410
411 The limits of the GAM method are most visible when large spans of data are missing; it is
412 essentially a smoothing technique, and has little predictive power (e.g. it cannot predict when missing
413 peaks may occur). However, this is also true for process-based models in most model validation
414 attempts, and the GAM provides an appropriate tool for imputing the missing observations in the
415 context of eddy covariance data. Significant improvements in our understanding of microbial
416 processes are still required to gap fill N₂O measurements with certainty.

417
418

419 N₂O Emission Factors

420 The EFs reported in this study varied widely, from 0.13 to 5.71 % of applied N. Although the IPCC
421 method assumes 1 % for all fertilisers (ranging from 0.03 to 3.0 %), EFs of up to 10 % as well as negative
422 values are reported from grasslands and agricultural fields (Charles et al., 2017), and the distribution
423 is log-normal (Stehfest & Bouwman, 2006).

424 In the UK, AN fertilisers are generally considered to emit more N₂O than urea based fertilisers,
425 although results based on experimentation has been inconsistent (Bell et al., 2015; Carswell et al.,
426 2018; Harty et al., 2016). For grasslands, the UK Agricultural Inventory (developed under the UK
427 agricultural emission factor, e.g. Brown et al. 2019) estimates EFs of 1.54 and 0.62 % for AN and urea,
428 respectively. In our experiment the mean EFs were 0.9 and 1.73 % for AN and urea fertiliser types,
429 respectively, but varied widely, from 0.13 to 5.71 %, and the difference was not statistically significant
430 ($p = 0.49$.) Given the difficulties of adequately sampling in space and time with chamber methods, it
431 has never been unequivocally clear whether the wide log-normal distribution of emission factors
432 observed was a result of sampling error, and whether genuine differences between fertiliser types
433 was lost amid the underlying heterogeneity.

434 Our study accurately quantifies EFs for multiple events and showing unambiguously that large-
435 scale temporal variability is real. That is, EFs do indeed vary from one fertiliser event to another, even
436 at the same site with the same fertiliser type under similar (though not identical) conditions. This
437 makes distinguishing EFs between different fertiliser types for the purposes of developing emission
438 mitigation policy very difficult, especially when the higher priority of economic risk is considered such
439 as impact on yield and farmer income. To estimate generic emission factors for different fertiliser
440 types in the UK (or any other region), a very large number of fertilisation events would need to be
441 measured to provide a robust comparison. In order to provide this comparison with practical
442 uncertainty values (i.e. $< \pm 0.25$ % of applied N), this is particularly challenging for chamber-based
443 approaches due to the amount of data collection required. Difficulties in assessing these differences
444 on a year to year basis are highlighted in this study by the possibility that 2 of the urea events may
445 have been influenced by decaying crop residue after harvest, and that the mean EF for urea if these 2
446 events were excluded would have been 0.43 % instead of 1.73 % (similar to what we might expect for
447 urea application in the region, reported as 0.29 ± 0.22 % in Cowan et al., 2019).

448 The wide variability in EFs and unpredictable behaviour in emissions after N application has
449 been attributed to a variety of reasons in the past, including fertiliser type, soil type, microbial
450 presence and environmental conditions (Maag & Vinther, 1996; Smith et al., 1998; Stevens et al., 1998;
451 Ball et al., 1999; Linn & Doran, 1984; Dobbie & Smith 2003). WFPS % was the environmental variable
452 with the most statistically significant correlation with N₂O fluxes in this study. The bell-curve

453 relationship between N₂O and WFPS peaking at 60 % WFPS has been described before in detail
454 (Davidson, 1993; Flechard et al., 2007). The relationship between soil moisture and rainfall with N₂O
455 emissions in this study is not as strong as in previous eddy covariance studies (Haszpra et al., 2018;
456 Liang et al., 2018), but this is likely due to the large number of variables in the soil changing with time,
457 the log-normal spatial variability of N₂O at the field scale and the random wind dependent spatial
458 coverage that the eddy covariance method measures from. Other studies examining the
459 environmental factors associated with N₂O emissions have measured closer to the surface (Congreves
460 et al., 2016; Wagner-Riddle et al., 2017); which may better represent the mass of soil in which the
461 microbiological processes are happening which contribute most to the land-atmosphere exchange of
462 N₂O.

463 In this study we used the available environmental data that is recorded by the adjacent
464 meteorological station to investigate for explaining variables in EFs, but these comparisons are limited
465 as they only provide fraction of information about what is occurring in the soil. We did not observe
466 any diurnal changes in N₂O flux during high or low emission periods, as has been reported in previous
467 eddy covariance studies in which it is suggested that temperature changes may affect N₂O emissions
468 (Liang et al., 2018). Finding a statistically significant correlation between EF and the WFPS % at the
469 time of fertilisation makes logical sense, as fertiliser pellets would be slow to dissolve into the soil
470 during dry periods (Chen et al., 2013). Correlation between EFs and rainfall prior to fertilisation events
471 has been made before at the Easter Bush site (Skiba et al., 2012), but the correlations observed in this
472 study are not convincing enough to say with certainty that this is a controlling variable in EF estimation.
473 As there is only a limited number of points from which to draw conclusions in this study (n = 10), we
474 do not believe the lack of strong correlation with variables is proof that environmental conditions are
475 not important. On the contrary, our study shows that there is a great deal of variability across the
476 events, and environmental factors must be the cause as very little else changes at the site during the
477 measurement years of 2012 to 2018.

478

479 Future considerations for N₂O flux studies

480 Although this study is unable to explain the reasons for the wide variability in EFs from different
481 fertiliser types, it provides evidence that our ability to measure and understand fluxes of N₂O at the
482 field scale is improving, primarily via the application of the eddy covariance method. Previously, it was
483 unsure if the wide ranging EFs reported in many chamber studies were real, or a result of
484 measurement uncertainties and interpolation of data spatially and temporally. This study shows that
485 even with almost constant data coverage, the reported fluxes still vary widely and unpredictably
486 between events. The most significant difficulty we predict when carrying out future studies is how

487 best to correlate soil properties and microbial activity at the field scale for comparison with eddy
488 covariance flux measurements. We know that the primary driver of anthropogenic N₂O emissions is
489 the availability of mineral nitrogen in soils (primarily NH₄⁺ and NO₃⁻); however, even mapping this
490 single driver (based on a handful of soil core measurements with no model by which to gap fill
491 spatially) to the footprint of an eddy covariance tower in a way that would allow significant statistical
492 correlation between flux and soil properties would be logistically difficult. As with N₂O flux (and many
493 other heterogeneous soil properties), available nitrogen in a field also follows a log-normal spatial and
494 temporal distribution (Cowan et al., 2015; Cowan et al., 2017) which means that a large number of
495 soil measurements at multiple depths would be required at regular time intervals (the collection of
496 which may even ruin the field site with constant trampling).

497 Microbial presence and activity is also vital to understand soil processes (Butterbach-Bahl et
498 al., 2013), and is prohibitively expensive, especially measured at the scale and high temporal rate that
499 eddy covariance would require for a robust comparison. For these reasons we consider the eddy
500 covariance method as a good way to provide data for the advancement of process based models and
501 verification of fertiliser emission factors; however, we do not recommend its use in experiments
502 attempting to advance understanding via controlled interactions between soil properties and N₂O
503 fluxes, which are probably better served by continuing incubation and plot scaled experiments using
504 flux chamber methodology.

505

506 **Conclusion:**

507 The EFs for N₂O reported in this study (cumulative flux over a period of 30 days after fertilisation) vary
508 from 0.13 to 5.71 % of applied nitrogen with EFs of 0.90 and 1.73 % for AN and urea fertiliser types,
509 respectively; however differences were not found to be statistically significantly due to the log-normal
510 distribution of the EF estimates. The study shows that similar applications of N can result in drastically
511 different emissions from the same field site in similar environmental conditions. More generally, given
512 that EFs can be so variable, we can conclude that detecting differences between fertiliser types or
513 other mitigation measures will be very challenging. The GAM provided a useful method able to fill the
514 gaps in flux data, using simple meteorological variables and provide uncertainties in cumulative flux
515 estimates.

516 **Acknowledgements**

517 Work was supported by the UK-China Virtual Joint Centre for Agricultural Nitrogen (CINAg,
518 BB/N013468/1), which is jointly supported by the Newton Fund, via UK BBSRC and NERC, and the
519 Chinese Ministry of Science and Technology with additional support for the site infrastructure from
520 NERC National Capability Funding, and the Natural Environment Research Council award number

521 NE/R016429/1 as part of the UK-SCaPE programme delivering National Capability. We also gratefully
522 acknowledge the invaluable help of farm manager Wim Bosma (Edinburgh University).

523 **References:**

524 Abalos, D., S.E. Brown, A.C. Vanderzaag, R.J. Gordon, K.E. Dunfield, et al. 2015. Micrometeorological
525 measurements over 3 years reveal differences in N₂O emissions between annual and perennial
526 crops. *Glob. Chang. Biol.*

527 Akiyama, H., Yan, X., Yagi, K., 2009. Evaluation of effectiveness of enhanced-efficiency fertilizers as
528 mitigation options for N₂O and NO emissions from agricultural soils: meta-analysis. *Global Change*
529 *Biology* 16, 1837–1846.

530 Bateman, E.J., Baggs, E.M., 2005. Contributions of nitrification and denitrification to N₂O emissions
531 from soils at different water-filled pore space. *Biology and Fertility of Soils* 41, 379–388.

532 Ball, B.C., Scott, A., Parker, J.P., 1999. Field N₂O, CO₂ and CH₄ fluxes in relation to tillage, compaction
533 and soil quality in Scotland. *Soil and Tillage Research* 53, 29–39.

534 Bell, M.J., Hinton, N., Cloy, J.M., Topp, C.F.E., Rees, R.M., Cardenas, L., Scott, T., Webster, C., Ashton,
535 R.W., Whitmore, A.P., Williams, J.R., Balshaw, H., Paine, F., Goulding, K.W.T., Chadwick, D.R., 2015.
536 Nitrous oxide emissions from fertilised UK arable soils: Fluxes, emission factors and mitigation.
537 *Agriculture, Ecosystems & Environment* 212, 134–147.

538 Brilli, L., Bechini, L., Bindi, M., Carozzi, M., Cavalli, D., Conant, R., Dorich, C.D., Doro, L., Ehrhardt, F.,
539 Farina, R., Ferrise, R., Fitton, N., Francaviglia, R., Grace, P., Iocola, I., Klumpp, K., Léonard, J., Martin,
540 R., Massad, R.S., Recous, S., Seddaiu, G., Sharp, J.,

541 Smith, P., Smith, W.N., Soussana, J.-F., Bellocchi, G., 2017. Review and analysis of strengths and
542 weaknesses of agro-ecosystem models for simulating C and N fluxes.

543 *Sci. Total Environ.* 598, 445–470.

544 BSFP (2017): The British Survey of Fertiliser Practice. Fertiliser use on farm crops for crop year 2016.
545 Defra, London. 99pp.

546 Butterbach-Bahl, K., Baggs, E.M., Dannenmann, M., Kiese, R., Zechmeister-Boltenstern, S., 2013.
547 Nitrous oxide emissions from soils: how well do we understand the processes and their controls?
548 *Philosophical Transactions of the Royal Society B: Biological Sciences* 368, 20130122–20130122.

549 Butler, J.H., Montzka, S.A. The NOAA annual greenhouse gas index (AGGI). NOAA Earth System
550 Research Laboratory, R/GMD, 325 Broadway, Boulder, CO 80305-3328, 2018; access 07/01/2019
551 <http://www.esrl.noaa.gov/gmd/aggi/aggi.html>

552 Carswell, A., Shaw, R., Hunt, J., Sánchez-Rodríguez, A.R., Saunders, K., Cotton, J., Hill, P.W., Chadwick,
553 D.R., Jones, D.L., Misselbrook, T.H., 2018. Assessing the benefits and wider costs of different N
554 fertilisers for grassland agriculture. *Archives of Agronomy and Soil Science* 1–15.

555 Chadwick, D.R., Cardenas, L., Misselbrook, T.H., Smith, K.A., Rees, R.M., Watson, C.J., McGeough, K.L.,
556 Williams, J.R., Cloy, J.M., Thorman, R.E., Dhanoa, M.S., 2014. Optimizing chamber methods for
557 measuring nitrous oxide emissions from plot-based agricultural experiments. *European Journal of*
558 *Soil Science* 65, 295–307.

559 Charles, A., Rochette, P., Whalen, J.K., Angers, D.A., Chantigny, M.H., Bertrand, N., 2017. Global nitrous
560 oxide emission factors from agricultural soils after addition of organic amendments: A meta-
561 analysis. *Agriculture, Ecosystems & Environment* 236, 88–98.

562 Chen, H.H., Li, X.C., Hu, F., Shi, W., 2013. Soil nitrous oxide emissions following crop residue addition:
563 a meta-analysis. *Global Change Biol.* 19, 2956–2964.

564 Congreves, K., S. Brown, D. Nemeth, K. Dunfield, and C. Wagner-Riddle. 2016. Differences in fieldscale
565 N₂O flux linked to crop residue removal under two tillage systems in cold climates. *Glob. Chang. Biol.*
566 *Bioenergy*.

567 Cowan, N.J., Norman, P., Famulari, D., Levy, P.E., Reay, D.S., Skiba, U.M., 2015. Spatial variability and
568 hotspots of soil N₂O fluxes from intensively grazed grassland.

569 Cowan, N.J., Levy, P.E., Famulari, D., Anderson, M., Drewer, J., Carozzi, M., Reay, D.S., Skiba, U.M.,
570 2016. The influence of tillage on N₂O fluxes from an intensively managed grazed grassland in
571 Scotland. *Biogeosciences* 13, 4811–4821.

572 Cowan, N.J., Levy, P.E., Famulari, D., Anderson, M., Reay, D.S., Skiba, U.M., 2017. Nitrous oxide
573 emission sources from a mixed livestock farm. *Agriculture, Ecosystems & Environment* 243, 92–
574 102.

575 Cowan, N., Helfter, C., Langford, B., Coyle, M., Levy, P., Moxley, J., Simmons, I., Leeson, S., Nemitz, E.,
576 Skiba, U., 2018. Seasonal fluxes of carbon monoxide from an intensively grazed grassland in
577 Scotland. *Atmospheric Environment* 194, 170–178.

578 Cowan, N., Levy, P., Drewer, J., Carswell, A., Shaw, R., Simmons, I., Bache, C., Marinheiro, J., Brichet,
579 J., Sanchez-Rodriguez, A.R., Cotton, J., Hill, P.W., Chadwick, D.R., Jones, D.L., Misselbrook, T.H.,
580 Skiba, U., 2019. Application of Bayesian statistics to estimate nitrous oxide emission factors of three
581 nitrogen fertilisers on UK grasslands. *Environment International* 128, 362–370.

582 Davidson, E.A., 1993. Soil Water Content and the Ratio of Nitrous Oxide to Nitric Oxide Emitted from
583 Soil, in: *Biogeochemistry of Global Change*. Springer US, pp. 369–386.

584 Davidson, E.A., Keller, M., Erickson, H.E., Verchot, L.V., Veldkamp, E., 2000. Testing a Conceptual
585 Model of Soil Emissions of Nitrous and Nitric Oxides. *BioScience* 50, 667.

586 Dobbie, K.E., Smith, K.A., 2003. Nitrous oxide emission factors for agricultural soils in Great Britain:
587 the impact of soil water-filled pore space and other controlling variables. *Global Change Biology* 9,
588 204–218.

589 Erisman, J.W., Sutton, M.A., Galloway, J., Klimont, Z., Winiwarter, W., 2008. How a century of ammonia
590 synthesis changed the world. *Nature Geoscience* 1, 636–639.

591 Finkelstein, P. L., and P. F. Sims. 2001. “Sampling Error in Eddy Correlation Flux Measurements.”
592 *Journal of Geophysical Research: Atmospheres* 106 (D4). Wiley-Blackwell: 3503–9.

593 Flechard, C. R., Ambus, P., Skiba, U., Rees, R. M., Hensen, A., van Amstel, A., Dasselaar, A. van den P.,
594 Soussana, J.-F., Jones, M., Clifton-Brown, J., Raschi, A., Horvath, L., Neftel, A., Jocher, M., Ammann,
595 C., Leifeld, J., Fuhrer, J., Calanca, P., Thalman, E., Pilegaard, K., Di Marco, C., Campbell, C., Nemitz,
596 E., Hargreaves, K. J., Levy, P. E., Ball, B. C., Jones, S. K., van de Bulk, W. C. M., Groot, T., Blom, M.,
597 Domingues, R., Kasper, G., Allard, V., Ceschia, E., Cellier, P., Laville, P., Henault, C., Bizouard, F.,
598 Abdalla, M., Williams, M., Baronti, S., Berretti, F. and Grosz, B. 2007. Effects of climate and
599 management intensity on nitrous oxide emissions in grassland systems across Europe, *Agric.*
600 *Ecosyst. Environ.*, 121(1–2), 135-152, doi:10.1016/j.agee.2006.12.024.

601 Foken, T.: 2003, *Angewandte Meteorologie, Mikrometeorologische Methoden*, Springer, Berlin,
602 Heidelberg, 289 pp.

603 Forster, P., Ramaswamy, V., Artaxo, P., Berntsen, T., Betts, R., Fahey, D. W., Haywood, J., Lean, J.,
604 Lowe, D. C., and Myhre, G.: Changes in atmospheric constituents and in radiative forcing. Chapter
605 2, in: *Climate Change 2007. The Physical Science Basis*, 2007.

606 Fratini, G., Ibrom, A., Arriga, N., Burba, G., Papale, D., 2012. Relative humidity effects on water vapour
607 fluxes measured with closed-path eddy-covariance systems with short sampling lines. *Agricultural*
608 *and Forest Meteorology* 165, 53–63.

609 Fuchs, K., Hörtnagl, L., Buchmann, N., Eugster, W., Snow, V., and Merbold, L.: Management matters:
610 testing a mitigation strategy for nitrous oxide emissions using legumes on intensively managed
611 grassland, *Biogeosciences*, 15, 5519-5543

612 Gelman, A. 2013. *Bayesian Data analysis*, 3rd edn. CRC Press, New York

613 Glenn, A.J., M. Tenuta, B.D. Amiro, S.E. Maas, and C. Wagner-Riddle. 2012. Nitrous oxide emissions
614 from an annual crop rotation on poorly drained soil on the Canadian Prairies. *Agric. For. Meteorol.*
615 166--167: 41–49.

616 Glibert, P.M., Harrison, J., Heil, C., Seitzinger, S., 2006. Escalating Worldwide use of Urea – A Global
617 Change Contributing to Coastal Eutrophication. *Biogeochemistry* 77, 441–463.

618 Harty, M.A., Forrestal, P.J., Watson, C.J., McGeough, K.L., Carolan, R., Elliot, C., Krol, D., Laughlin, R.J.,
619 Richards, K.G., Lanigan, G.J., 2016. Reducing nitrous oxide emissions by changing N fertiliser use
620 from calcium ammonium nitrate (CAN) to urea based formulations. *Science of The Total*
621 *Environment* 563–564, 576–586.

622 Haszpra, L., Hidy, D., Taligás, T., Barcza, Z., 2018. First results of tall tower based nitrous oxide flux
623 monitoring over an agricultural region in Central Europe. *Atmospheric Environment* 176, 240–251.

624 IPCC, 2014: Climate Change 2014: Synthesis Report. Contribution of Working Groups I, II and III to the
625 Fifth Assessment Report of the Intergovernmental Panel on Climate Change [Core Writing Team,
626 R.K. Pachauri and L.A. Meyer (eds.)]. IPCC, Geneva, Switzerland, 151 pp.

627 Ibrom, A., Dellwik E., Flyvbjerg H., Jensen N. O., and Pilegaard K., 2007. “Strong Low-Pass Filtering
628 Effects on Water Vapour Flux Measurements with Closed-Path Eddy Correlation Systems.”
629 *Agricultural and Forest Meteorology* 147 (3-4). Elsevier BV: 140–56.

630 Jones, S.K., Famulari, D., Di Marco, C.F., Nemitz, E., Skiba, U.M., Rees, R.M., Sutton, M.A., 2011. Nitrous
631 oxide emissions from managed grassland: a comparison of eddy covariance and static chamber
632 measurements. *Atmospheric Measurement Techniques* 4, 2179–2194.

633 Jones, S., Helfter, C., Anderson, M., Coyle, M. Campbell, C., Famulari, D., Di Marco, C. et al. 2017. “The
634 Nitrogen, Carbon and Greenhouse Gas Budget of a Grazed, Cut and Fertilised Temperate
635 Grassland.” *Biogeosciences* 14 (8). Copernicus GmbH: 2069–88.

636 Köhli, M., M. Schrön, M. Zreda, U. Schmidt, P. Dietrich, and S. Zacharias. 2015. “Footprint
637 Characteristics Revised for Field-Scale Soil Moisture Monitoring with Cosmic-Ray Neutrons.” *Water
638 Resources Research* 51 (7). Wiley-Blackwell: 5772–90.

639 Kroon, P.S., Hensen, A., Jonker, H.J.J., Ouwensloot, H.G., Vermeulen, A.T., Bosveld, F.C., 2010.
640 Uncertainties in eddy covariance flux measurements assessed from CH₄ and N₂O observations.
641 *Agricultural and Forest Meteorology* 150, 806–816.

642 Lehuger, S., Gabrielle, B., Oijen, M. van, Makowski, D., Germon, J. C., Morvan, T., Hénault, C., 2009.
643 Bayesian calibration of the nitrous oxide emission module of an agro-ecosystem model.
644 *Agriculture, Ecosystems & Environment* 133, 208–222.

645 Levy, P.E., Cowan, N., van Oijen, M., Famulari, D., Drewer, J., Skiba, U., 2017. Estimation of cumulative
646 fluxes of nitrous oxide: uncertainty in temporal upscaling and emission factors. *European Journal
647 of Soil Science* 68, 400–411.

648 Liang, L.L., Campbell, D.I., Wall, A.M., Schipper, L.A., 2018. Nitrous oxide fluxes determined by
649 continuous eddy covariance measurements from intensively grazed pastures: Temporal patterns
650 and environmental controls. *Agriculture, Ecosystems & Environment* 268, 171–180.

651 Linn, D.M., Doran, J.W., 1984. Effect of Water-Filled Pore Space on Carbon Dioxide and Nitrous Oxide
652 Production in Tilled and Nontilled Soils¹. *Soil Science Society of America Journal* 48, 1267.

653 Maag, M., Vinther, F., 1996. Nitrous oxide emission by nitrification and denitrification in different soil
654 types and at different soil moisture contents and temperatures. *Applied Soil Ecology* 4, 5–14.

655 Mammarella, I., Werle, P., Pihlatie, M., Eugster, W., Haapanala, S., Kiese, R., Markkanen, T., Rannik,
656 Ü., Vesala, T., 2010. A case study of eddy covariance flux of N₂O measured within forest
657 ecosystems: quality control and flux error analysis. *Biogeosciences* 7, 427–440.

658 Marra, G., Wood, S.N., 2012. Coverage Properties of Confidence Intervals for Generalized Additive
659 Model Components. *SCANDINAVIAN JOURNAL OF STATISTICS* 39, {53-74}.

660 Merbold, L., Eugster, W., Stieger, J., Zahniser, M., Nelson, D., Buchmann, N., 2014. Greenhouse gas
661 budget (CO₂, CH₄ and N₂O) of intensively managed grassland following restoration. *Global Change*
662 *Biology* 20, 1913–1928.

663 Moncrieff, J.B., Massheder, J.M., de Bruin, H., Elbers, J., Friborg, T., Heusinkveld, B., Kabat, P., Scott,
664 S., Soegaard, H., Verhoef, A., 1997. A system to measure surface fluxes of momentum, sensible
665 heat, water vapour and carbon dioxide. *Journal of Hydrology* 188–189, 589–611.

666 Ravishankara, A.R., Daniel, J.S., Portmann, R.W., 2009. Nitrous Oxide (N₂O): The Dominant Ozone-
667 Depleting Substance Emitted in the 21st Century. *Science* 326, 123–125.

668 Robertson, G.P., Tiedje, J.M., 1987. Nitrous oxide sources in aerobic soils: Nitrification, denitrification
669 and other biological processes. *Soil Biology and Biochemistry* 19, 187–193.

670 Rochette, P., Worth, D.E., Lemke, R.L., McConkey, B.G., Pennock, D.J., Wagner-Riddle, C., Desjardins,
671 R.J., 2008a. Estimation of N₂O emissions from agricultural soils in Canada. I: Development of a
672 country specific methodology. *Can. J. Soil Sci.* 88, 641–654

673 Rochette, P., Eriksen-Hamel, N.S., 2008b. Chamber Measurements of Soil Nitrous Oxide Flux: Are
674 Absolute Values Reliable? *Soil Science Society of America Journal* 72, 331.

675 Skiba, U., Jones, S.K., Dragosits, U., Drewer, J., Fowler, D., Rees, R.M., Pappa, V.A., Cardenas, L.,
676 Chadwick, D., Yamulki, S., Manning, A.J., 2012. UK emissions of the greenhouse gas nitrous oxide.
677 *Philosophical Transactions of the Royal Society B: Biological Sciences* 367, 1175–1185.

678 Smith, K., Thomson, P., Clayton, H., McTaggart, I., Conen, F., 1998. Effects of temperature, water
679 content and nitrogen fertilisation on emissions of nitrous oxide by soils. *Atmospheric Environment*
680 32, 3301–3309.

681 Smith, K.A., McTaggart, I.P., Tsuruta, H., 1997. Emissions of N₂O and NO associated with nitrogen
682 fertilization in intensive agriculture, and the potential for mitigation. *Soil Use and Management* 13,
683 296–304.

684 Stehfest, E., Bouwman, L., 2006. N₂O and NO emission from agricultural fields and soils under natural
685 vegetation: summarizing available measurement data and modeling of global annual emissions.
686 *Nutrient Cycling in Agroecosystems* 74, 207–228.

687 Stevens, R.J., Laughlin, R.J., Malone, J.P., 1998. Soil pH affects the processes reducing nitrate to nitrous
688 oxide and di-nitrogen. *Soil Biology and Biochemistry* 30, 1119–1126.

689 Tilman, D., Cassman, K.G., Matson, P.A., Naylor, R., Polasky, S., 2002. Agricultural sustainability and
690 intensive production practices. *Nature* 418, 671–677.

691 Vesala, T., Kljun, N., Rannik, Ü., Rinne, J., Sogachev, A., Markkanen, T., Sabelfeld, K., Foken, T., Leclerc,
692 M.Y., 2008. Flux and concentration footprint modelling: State of the art. *Environmental Pollution*
693 152, 653–666.

694 Wagner-Riddle, C., A. Furon, N.L. McLaughlin, I. Lee, J. Barbeau, et al. 2007. Intensive Management of
695 nitrous oxide emissions from a corn-soybean-winter-wheat rotation under two contrasting
696 management systems over 5 years. *Glob. Chang. Biol.* 13: 1722–1736.

697 Wagner-Riddle, C., K.A. Congreves, D. Abalos, A.A. Berg, S.E. Brown, et al. 2017. Globally important
698 nitrous oxide emissions from croplands induced by freeze-thaw cycles. *Nat. Geosci.* 10(4). doi:
699 10.1038/ngeo2907.

700 Waldo, S., E.S. Russell, K. Kostyanovsky, S.N. Pressley, P.T. O’Keeffe, et al. 2019. N₂O Emissions From
701 Two Agroecosystems: High Spatial Variability and Long Pulses Observed Using Static Chambers
702 and the Flux-Gradient Technique. *J. Geophys. Res. Biogeosciences* 124(7): 1887– 1904.

703 Wood, S. N.: *Generalized additive models: an introduction with R*, Chapman & Hall/CRC, Boca Raton,
704 FL., 2006.